Int. J. Electrochem. Sci., 12 **(2017)** 12019 – 12036, doi: 10.20964/2017.12.35

International Journal of
ELECTROCHEMICAL
SCIENCE
www.electrochemsci.org

Glassy Carbon Electrode Modified with Gold nanoparticles/thiol-β-cyclodextrin—graphene for the Determination of Nonylphenol

Wen Chen[1,2,*], *Yuting Jiang*[1,2], *Fei Xue*[3*], *Tingting Zhang*[1,2]

[1] 1.College of Materials and Chemistry & Chemical Engineering, Chengdu University of Technology, Chengdu, Sichuan 610059, People's Republic of China
[2] Mineral Resources Chemistry Key Laboratory of Sichuan Higher Education Institution, Chengdu, Sichuan 610059, People's Republic of China
[3]Xi'an Medical College, Xian, Shanxi 710000, People's Republic of China
[*]E-mail: chenwen2010@foxmail.com, xuefei051@foxmail.com

Received: 6 September 2017 / *Accepted:* 22 October 2017 / *Published:* 12 November 2017

The gold nanoparticles (AuNPs) was firstly polymerized on the surface of glassy carbon electrode (GCE) using the chronoamperometry, then the gold nanoparticles/thiol-β-cyclodextrin–graphene/GCE (AuNPs/SH-β-CD—GR/GCE) was directly synthesized with the complex of thiol-β-cyclodextrin (SH-β-CD) and graphene oxide (GO) by cyclic voltammetry (CV). The AuNPs/SH-β-CD—GR/GCE was characterized by field emission scanning electron microscopy (FESEM), which indicated that the as-polymerized Au nanoparticles were successfully dispersed on the surface of GCE and combined with SH-β-CD and GR. Simultaneously, the electrochemical behavior of nonylphenol (NP) was investigated by CV and differential pulse voltammetry (DPV). The oxidation current of NP on AuNPs / SH-β-CD-GR / GCE is much higher than that of GCE, AuNPs / GCE and AuNPs / GR / GCE, and the oxidation potential is shifted negatively, it indicates that the NP has been apparently catalyzed by AuNPs / SH-β-CD-GR/GCE. The conditions of preparation and test were optimized, on the condition of optimization, the oxidation current is linearly proportional to the concentration of NP over the range of 0.05 ~ 50μmol L^{-1} (R = 0.9901), the detection limit is 0.017μmolL^{-1} (($P < 0.05$) S / N = 3). The recoveries of samples are from 96.11% to 105.9%. The result is satisfactory when it is used to analyze the real samples.

Keywords: gold nanoparticles; graphene; thiol-β-cyclodextrin; nonylphenol

1. INTRODUCTION

Nonylphenol（NP） is an important chemical raw material and intermediate [1], which widely used in surface active agent, antioxidant, textile printing, dyeing additives, lubricating oil additive, and resin and rubber stabilizer. Meanwhile, NP is an important environmental toxicant and potential endocrine disrupting chemical [2]. Due to the environmental xenoestrogenic effects and bioaccumulation of NP, once the NP is released into the environment, it will accumulated in the organism and cause serious impact on the reproductive system and development ability of the organism, which known as a "killer sperm"[3,4]. Therefore, it is necessary to develop a rapid, simple, and efficient method for the determination of NP. It was reported that the main methods used for the determination of NP included gas chromatography (GC)[5], liquid chromatography(LC)[6], high performance liquid chromatography(HPLC)[7], gas chromatography/liquid chromatography coupled with mass spectrometry(GC/LC–MS)[8,9], immunosensors[10]and electrochemical sensors. Among these analytical methods, electrochemical sensor had the advantage of rapid response, low cost, simple operation, time saving, high sensitivity and real-time detection [11, 12]. However, due to the high overpotential and poor sensitivity of bare electrode for the determination of NP, it is essential to develop a composite film-modified electrode to extend the dynamic range of analytical determination of electrochemical sensor and decrease the detection limit [13].

Currently, a number of electrochemical sensors have been reported for the determination of NP. These sensors are mainly the following types: one is the NP sensor with molecularly imprinted functionalized substrate electrode. For instance, Huang et al. [14] detected 4-NP using a 4-NP-imprinted functionalized AuNPs composites modified glassy carbon electrode (GCE) with a detection limit (LOD) of 0.32μmolL^{-1}. Zhang and his co-workers [15] developed a sensitive and selective detection technique for 2-NP determination based on a multi-walled carbon nanotubes–Nafion (MWNT/NF) molecularly imprinted film modified the GCE (MWNT/NF/GCE), which LOD was 0.06μmolL^{-1}. Pan et al. [16] constructed a novel electrochemical sensor based on molecularly imprinted poly (o-phenylenediamine-o-o-toluidine) nitrogen-doped graphene nanocarbon ionic liquid composite membrane (NGNRs-IL / GCE) for the determination of NP. This sensor has a good anti-interference, because the analyte can be selectively combined with the imprinting hole. The second type of sensor is a composite biosensor. A novel electrochemical sensor, which was sensitive to NP detection, was prepared based a reduced graphene–DNA hybrid-modified GCE (GR-DNA/GCE) by Nan et al. [17]. The sensor utilizes the specificity and the better selectivity of aptamer, but the selection of DNA aptamer is more complex, so this type of sensor is less reported. The third type of sensor is made of metal nanomaterial, graphene, carbon nanotubes and other materials. Such sensors because of more types of modified materials and modification methods are more reported. For example, Meng et al. [18] detected the NP using ionic liquid-functionalized graphene nanosheet modified GCE ($FGNS^{IL}$ / GCE). Zheng et al. [19] prepared a sensor based on gold nanoparticles/multi-walled carbon nanotubes modified GCE (AuNPs-CNTs /GCE) for the determination of 4-NP. Xue et al. [20] prepared a thiol-β-cyclodextrin (β-CD-SH) and graphene (GR) hybrid-modified gold electrode (β-CD-SH—GR/Au) for the electrochemical detection of NP. Ma et al. [21] proposed a palladium nanoparticles supported on poly (diallyl dimethyl ammonium chloride)-mesoporous carbon (Pd/PDDA-MC) modified GCE (Pd/PDDA-MC/GCE) for NP oxidation. And the electrochemical sensor based on a nanocomposite consisting of cetyltrime-thylammonium bromide (CTAB), Fe_3O_4 nanoparticles and reduced graphene oxide (CTAB-Fe_3O_4 -rGO) modified GCE (CTAB-Fe_3O_4-rGO/GCE) for NP detection was prepared by Zou et al. [22]. Ren and his co-workers [23] developed a novel electrochemical sensor of 4-NP based on a poly (ionic liquid) hollow nanosphere/gold nanoparticle composite modified GCE

(AuNP/PIL/GCE). These kinds of sensor combine the advantages of various materials, such as excellent conductivity and easy connection with analyte, so the sensitivity and range of detection are relatively good. Another type of sensor is the modified screen-printed carbon electrode. For example, a novel assay for the electrochemical detection of 4-NP based on carbon nanotubes modified screen-printed carbon electrodes (CNTs-SPCEs) has been investigated by Buleandra et al.[24]. This type of sensor using disposable screen-printed electrode has the advantages of being free of regeneration and contamination, but they also have the problems of the consistency of the electrodes and the green recovery of the waste electrodes. In view of the high cost of electrode detection, there are few related studies at present. In summary, the novel test method for the determination of NP based on AuNPs/SH-β-CD—GR modified GCE (AuNPs/SH-β-CD—GR/GCE) has not been reported.

Nowadays, gold nanoparticles (AuNPs) have become very popular materials for modification of the electrochemical sensors and biosensors due to large specific surface area, high catalytic activity, small size, good biocompatibility, strong adsorption ability and good conductivity [25-27]. On the other hand, Graphene (GR), the new nanocarbon material with a unique structure of single atom and a large two-dimensional plane, has generated great interest and gained popularity on electrochemical sensor fabrication due to its properties of large surface, unusual electronic transport, excellent electrical conductivity, and super catalytic activity[28-31]. Moreover, cyclodextrin(CD) and its derivatives have a hollow cylindrical structure,which have the properties of inner hydrophobic and outer hydrophilic. And β- cyclodextrin(β-CD) is a cyclic oligosaccharide consisting of seven glucose units, which often used as a dispersing reagent for the insoluble chemicals and nanomaterials and exhibits excellent film-forming ability and inclusion function[32,33].Meanwhile, β-CD can form host-guest complexes with a number of inorganic ions, organic molecules, biological pesticides drugs and other small molecules due to its high selectivity, recognition and preconcentration[34-36]. In this paper, the thiol- functional β-cyclodextrin (β-CD-SH) was selected as another ideal electrode material as the Au-S bond has better stability. Considering respective advantages of GR, AuNPs and β-CD-SH ， the composite film exhibits good synergistic effect between each other and unique electrochemical traits for the redox reaction of NP. Preparation of AuNPs / SH-β-CD-GR / GCE and detection mechanism of NP can be explained as follows: the AuNPs was deposited on the surface of GCE by electrochemical reduction, and the hydroxyl groups of GO connect β-CD-SH Hydroxyl groups with hydrogen bonds, after electrochemical reduction, the epoxy and carboxyl groups of GO were disappeared, only hydroxyl left combining with β-CD-SH, SH-β-CD forms stable Au-S bond with AuNPs on the surface of GCE, in addition the intermolecular hydrogen bonds of NP and β-CD-SH can weaken the oxygen-hydrogen bond of NP, which is beneficial to the oxidation of NP (Fig.1)

In this work, AuNPs/SH-β-CD—GR/GCE is prepared, and the preparation method, the electrochemical behavior and the voltammetric determination of NP in the modified electrode are presented.

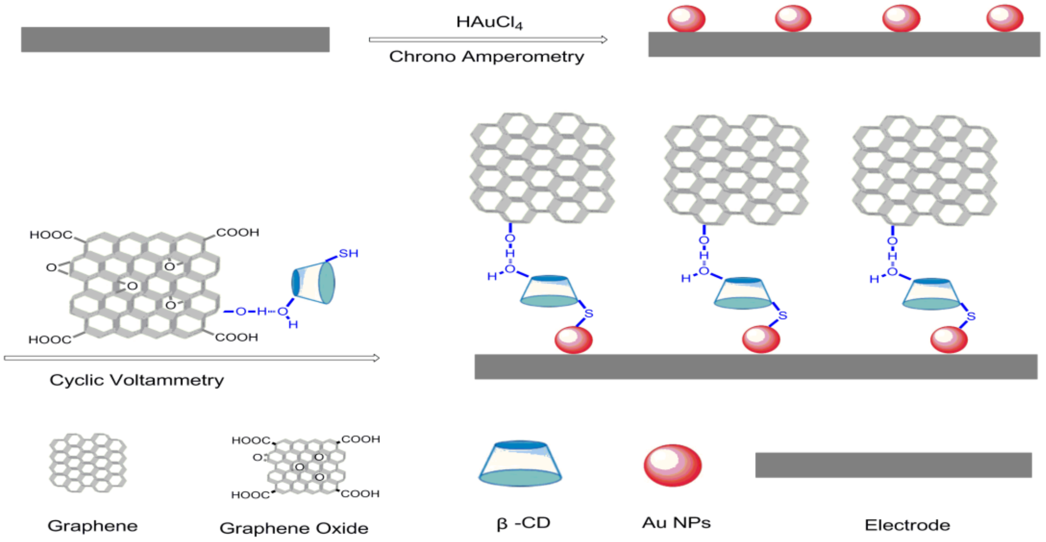

Figure 1. The procedure for the formation of the AuNPs/SH-β-CD—GR/GCE and detection mechanism of NP.

2. MATERIALS and METHODS

2.1 Reagents and instruments

PGSTAT302N electrochemical workstation (metrohm Co.,Ltd.,China); Quanta250 FEG field emission scanning electron microscope (FEI, China).Nonylphenol was purchased from Guangfu Fine Chemical Research Institute (Tianjin, China); thiol-β-cyclodextrin was obtained from Binzhou Zhiyuan Bio-Technology Co.,Ltd. (Shandong,China); chloroauric acid tetrahydrate ($HAuCl4\cdot4H_2O$) was bought from KeLong Chemical; graphite powder (spectroscopically pure SP); graphene oxide (GO) was prepared according to the literature method using graphite powder. All solutions were prepared in double-distilled water; all other reagents were of analytical grade.

2.2 Preparation of the modified electrodes

Prior to electrodeposition, the surface of GCE was polished with 1.0μm, 0.3μm and 0.05μm alumina powders successively, and then sonicated in anhydrous ethanol and double-distilled water, respectively. Firstly, the cleaned GCE was immersed into 1mM chloroauric acid ($HAuCl_4$) solution containing 0.1M sodium sulfate (Na_2SO_4) solution as electrolyte, and the gold nanoparticles (AuNPs) were electrodeposited at a constant potential of -0.8V for 100s by the chronoamperometry. Then removed the electrode from the solution, washed the surface carefully with double-distilled water and dried under the nitrogen stream, which was AuNPs/GCE. Secondly, the prepared AuNPs/GCE was immersed into 3mg·mL^{-1} GO and β-CD-SH—GO ($C_{\beta\text{-CD-SH}}$: CGO=1:3) suspension, respectively. Then the GO and β-CD-SH—GO were reduced on the surface of AuNPs/GCE by cyclic voltammetry within the potential window of −1.4-0.6 V (vs. SCE) for 12 cycles, which scan rate was 100mv/s. The obtained electrodes were denoted as AuNPs/GR/GCE and AuNPs/SH-β-CD—GR/GCE.

3. RESULTS and DISCUSSION

3.1 Optimization of preparation conditions of AuNPs/SH-β-CD—GR/GCE

3.1.1 The solvent and concentration of $HAuCl_4$ solution

In this experiment, the effect of different solvents on the response of the modified electrode was investigated (Table 1). It was found that compared with 0.1M KCl, the peak current of the modified electrode was larger when the 0.1M Na_2SO_4 as the solvent of $HAuCl_4$. At the same time, the concentration of $HAuCl_4$ solution was also studied (Table.2). The modified electrode was prepared in 0.1, 1, 10mM $HAuCl_4$ solution, separately. When the concentration of $HAuCl_4$ was 1mM, the peak current was the maximum. When the concentration of $HAuCl_4$ was 10mM, the peak current decreased obviously, this phenomenon indicated that when the concentration of $HAuCl_4$ was too large, the modification amount of nano-gold was excessively, which resulted in the decrease of electrode conductivity; therefore, the optimized concentration of $HAuCl_4$ was 1mM.

In the literature [19], the gold nanoparticles were modified on the surface of electrode using 0.5mmol/L $HAuCl_4$ aqueous solution without electrolyte solution, and the effect of concentration was not discussed. In this study, the solvent and concentration of $HAuCl_4$ were selected according to the literatures [37, 38], and the results are consistent with them. Therefore, electrodeposition at this concentration, the thickness of the gold nanoparticles on the surface of the GCE is most favorable for the electron conduction.

Table 1. The effect of solvent on the peak current of NP

solvent（0.1mol/L）	KCl	Na_2SO_4
I_p（μA）	0.52168	0.42542

Table 2. The effect of concentration of $HAuCl_4$ on the peak current of NP

C_{HAuCl_4}（mM）	0.1	1	10
I_p（μA）	0.47650	0.52168	0.23984

3.1.2 The reduction potential of AuNPs

The AuNPs/GCE was prepared under the reduction potential of -0.2V、-0.4V、-0.8V and -0.9V, respectively (**Figure** 2). When the reduction potential of gold nanoparticles was -0.8V， the peak current was the maximum. While the potential was negative than -0.8V or positive than -0.4V, the peak current significantly decreased. So, -0.8 V was selected as the optimal reduction potential of AuNPs .

In the literatures [19,37], the reduction potential of gold nanoparticles was -0.2V，and they had no discussion about the selection of the reduction potential. On the basis of the literature, the reduction potential of this study was discussed in a wide range, but the results obtained in the end were quite different from those reported in the literature. This may be caused by different reducing medium, the acidity of the reducing medium in the literature[37](0.01 mol L^{-1} Na_2SO_4 and 0.01 mol L^{-1} H_2SO_4) was relatively high, while the acidity in this paper was lower.

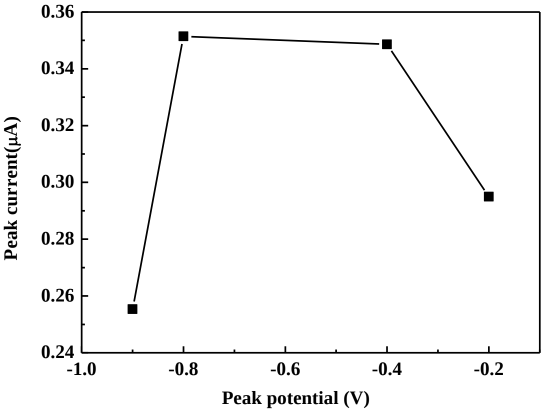

Figure 2 The reduction potential of AuNPs on the peak current of NP
(The modified electrode was made of 1mM $HAuCl_4$ in 0.1M Na_2SO_4 , $C_{β\text{-CD-SH}}$:C_{GO}=10 mg·mL^{-1}:30 mg·mL^{-1}(1:3), 100s by the chronoamperometry, within the potential window of −1.4-0.6 V (vs. SCE) for 12 cycles, scan rate was 100mv/s.)

3.1.3 The electrodeposition ime of AuNPs

Under the electrodeposition time of 100, 200, 300, 400s, the effect on the peak current was studied respectively. It was found that the peak current gradually decreased with the extension of time. It is possible that AuNPs film has thickened and prevented the conduction of electrons.Therefore, the optimum deposition time was 100 seconds.

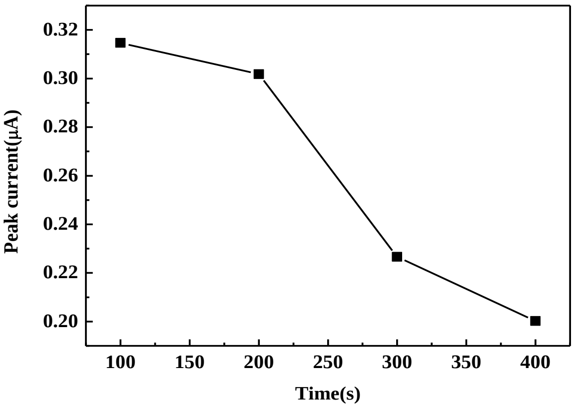

Figure 3 The reduction time of AuNPs on the peak current of NP
(The modified electrode was made of 1mM $HAuCl_4$ in 0.1M Na_2SO_4 , $C_{β\text{-CD-SH}}$:C_{GO}=10 mg·mL^{-1}:30 mg·mL^{-1}(1:3), -0.8V (vs. SCE) by the chronoamperometry, within the potential window of −1.4-0.6 V (vs. SCE) for 12 cycles, scan rate was 100mv/s.)

In the literatures [19,37], the electrodeposition time were 180s and 30s, respectively, but they had no detailed discussion about the selection of the polymerization time. On the basis of the literature, the electrodeposition time in this paper was discussed in a certain range, but the research result was not consistent with the literatures, which may also be caused by the acidity of the reducing medium .

3.1.4 The ratio of β-CD-SH to GO

The affinity and conductivity of the modified electrode are affected by the mass ratio of of *β-CD-SH to GO* in the electropolymerization process. A series of different mass ratios of 1:1, 1:3, 1:5, 1:8, 1:10 of β-CD-SH to GO dispersions were prepared respectively. With the increase of mass ratio, the peak current increased gradually and reached highest in 1:3. However, when the ratio was higher than 1:3, the peak current went down. Therefore, the ratio of 1:3 was selected as the optimum for the peak current increased significantly. Although the graphene can increase the conductivity of the electrode, too much graphene oxide in solution will make the deposited graphene of the surface too thick, and decrease the conductivity of the electrode.

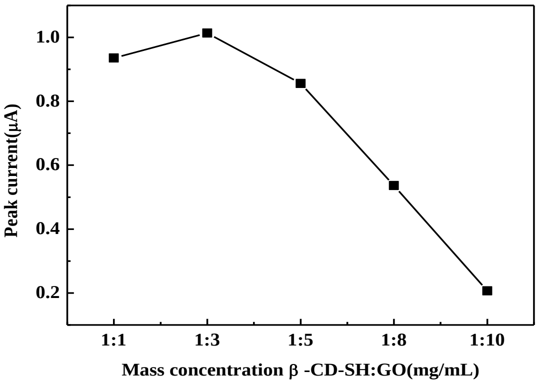

Figure 4 The ratio of β-CD-SH and GO on the peak current of NP (The modified electrode was made of 1mM $HAuCl_4$ in 0.1M Na_2SO_4, -0.8V (vs. SCE) for 100s by the chronoamperometry, within the potential window of −1.4-0.6 V (vs. SCE) for 12 cycles, scan rate was 100mv/s.)

3.1.5 The reduction cycle of β-CD-SH and GO

In this experiment, the reduction cycles of β-CD-SH and GO dispersion was also studied, and the AuNPs/SH-β-CD—GR/GCE was prepared in different reduction cycles of 6, 12, 18 and 24, respectively (**Figure** 5) When the reduction cycles were less than 12, the peak current was improved with the increase of the cycles. However, more than 12 cycles will result in a decrease in peak current. This was because when the reduction cycle was less, only part of GO was reduced. Nevertheless, the more reduction cycle could increase the thickness of the film and reduce its conductivity. Therefore, the optimized reduction cycles were 12.

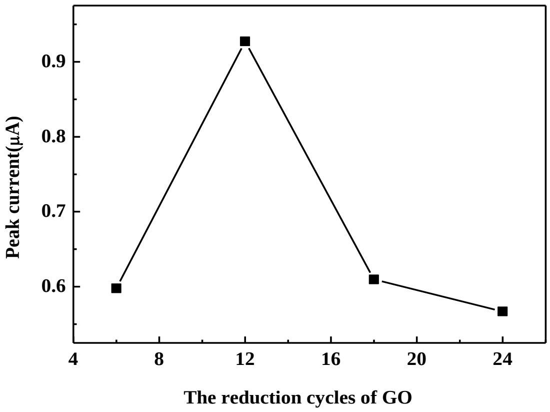

Figure 5 The reduction cycle of β-CD-SH and GO on the peak current of NP (The modified electrode was made of 1mM $HAuCl_4$ in 0.1M Na_2SO_4, $C_{β\text{-CD-SH}}$:C_{GO}=10 mg·mL^{-1}:30 mg·mL^{-1}(1:3), -0.8V (vs. SCE) for 100s by the chronoamperometry, within the potential window of −1.4-0.6 V (vs. SCE), scan rate was 100mv/s.)

3.2 Electrochemical Behavior of modified electrode

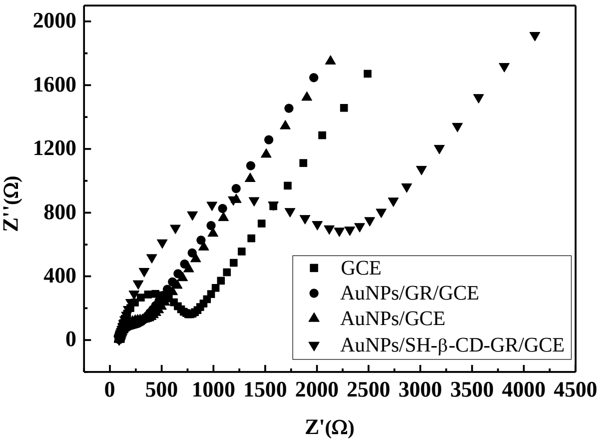

Figure 6. Electrochemical impedance spectroscopy (EIS) of GCE, AuNPs/GCE, AuNPs/GR/GCE and AuNPs/SH-β-CD—GR/GCE (initial potential: 0.2 V, Frequency: 10^{-2}-10^{5}Hz)

The properties of the modified electrode were characterized by electrochemical impedance spectroscopy (EIS) and field emission scanning electron microscopy (FESEM).The electrical properties of the different modified films can be effectively evaluated by electrochemical impedance spectroscopy (EIS). The Nyquist diagram contains a semicircular part and linear segment, and the low frequency linear segment shows a controlled diffusion process, and the high frequency semicircular part corresponds to the electron transfer restriction process. Meanwhile, the diameter of the semicircle represents the electron transfer resistance. Figure 6 clearly shows the semicircular and linear characteristics of the Nyquist graphs of bare GCE, AuNPs / GCE, AuNPs / GR / GCE and AuNPs /

SH-β-CD-GR / GCE. Due to the good conductivity of AuNPs, the resistance of AuNPs / GCE is lower than that of bare GCE.

When the AuNPs/GCE compounded with GR, the resistance value of AuNPs/GR/GCE was lower, which is ascribed to GR also has excellent electrical conductivity and has a synergistic effect with AuNPs. However, for the AuNPs/SH-β-CD-GR/GCE, there is a large well-defined arc in the high frequency region, which is ascribed to the nonconducting β-CD-SH increase the charge transfer resistance. Meanwhile, it also indicated that the β-CD-SH was successfully modified on the electrode.

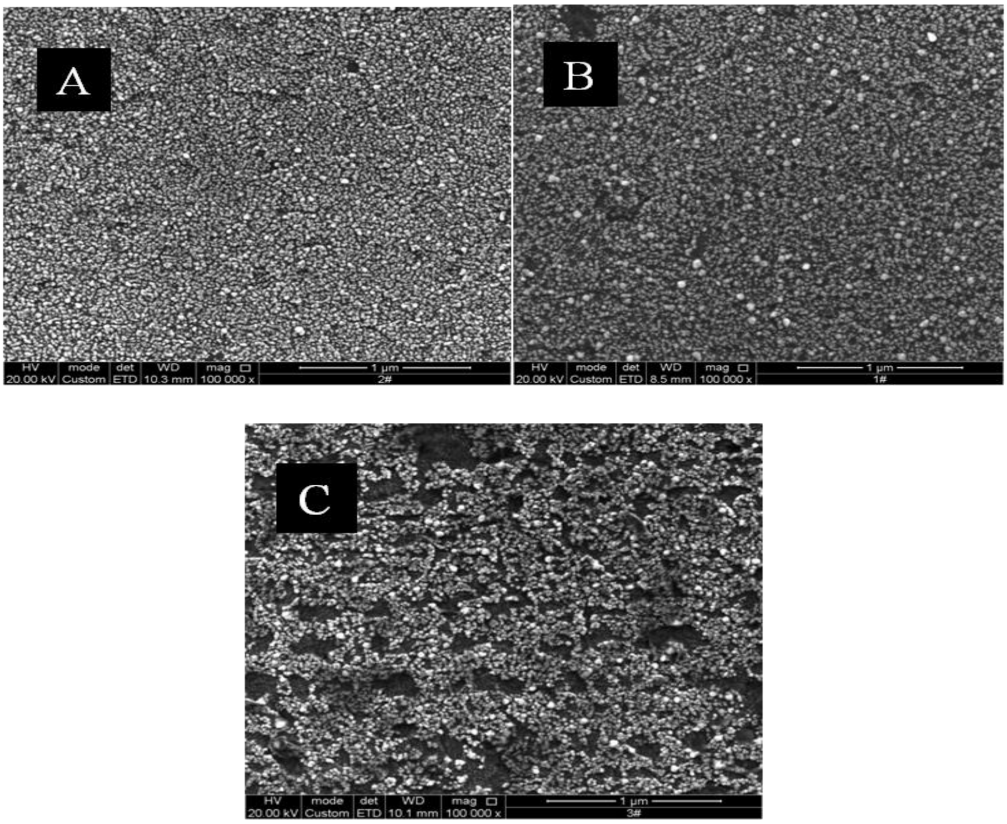

Figure 7. The FESEM image of the AuNPs/GCE (**A**), AuNPs/GR/GCE (**B**) and AuNPs/SH-β-CD-GR/GCE（**C**）

The morphology of the prepared AuNPs/GCE、AuNPs/GR/GCE and AuNPs/SH-β-CD-GR/GCE were characterized by FESEM without gold spraying because of good conductivity of Au and GR (as shown in Figure 7A), AuNPs evenly deposited on the electrode surface showed a significant metallic sheen, the deposition potential and deposition time controlling AuNPs size. On the conditions of optimum deposition, the diameter of AuNPs is between 10 nm and 50 nm. Meanwhile, FIG. 7B is a FESEM image showing a fine structure of AuNPs / GR / GCE, which the dense of AuNPs combining with GR could be observed and the gloss reduction than AuNPs due to the GR without luster, it shows that AuNPs and GR had been deposited on the surface of GCE.

Moreover, when the SH-β-CD was modified on the surface of AuNPs/GR/GCE, the morphology of AuNPs/SH-β-CD-GR/GCE (Figure 2C) was greatly changed and there were some shaded area because of non-electric conductivity of SH-β-CD, the feature is the same as the EIS, Thus, the preparation of AuNPs / SH-β-CD-GR / GCE was successful.

3.3 The electrochemical behavior of NP on different modified electrodes

The cyclic voltammograms of the NP of the four electrodes are shown in Fig. 8, and it can be seen that there is only an oxidation peak on all the electrodes without a corresponding reduction peak, indicating that the electrode reaction of NP is completely irreversible.

In addition, compared with GCE（0.627V），AuNPs/GCE（0.615V）and AuNPs/GR/GCE（0.574V）, Because GR and AuNP have large surface area and high electrocatalytic activity, the peak potential of AuNPs / SH-β-CD-GR / GCE (0.569V) is negatively shifted, Meanwhile, the oxidation peak current of NP on AuNPs/SH-β-CD—GR/GCE (I_{pa} =1.1126μA) is about 5.39，2.16 and 2.01 times higher than that of the GCE（Ipa=0.2064）, AuNPs/GCE（I_{pa}= 0.5159）and AuNPs/GR/GCE（I_{pa}= 0.5524）, respectively, which indicating that β-CD-SH has excellent recognition and connectivity to NP, and the AuNPs and GR provide high conductivity, Moreover, the three have a good synergistic effect in this process.

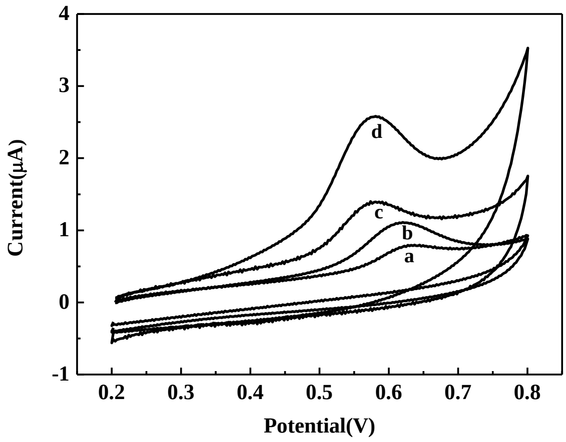

Figure8. The electrochemical behavior of GCE（**a**）, AuNPs/GCE（**b**）, AuNPs/GR/GCE（**c**）, AuNPs/SH-β-CD—GR/GCE (**d**) in PBS (pH6.0) containing 1.0×10^{-5}mol L^{-1}NP.

3.4 Optimization of AuNPs / SH- beta -CD-GR / GCE test conditions

3.4.1 Optimization of electrolyte and pH

Compared with HAc-NaAc and citric acid-sodium citrate (CA-SC) buffer solution, It can be seen that the peak current response value of NP in PBS is the largest, the peak potential shifted negatively. At the same time, the pH value of PBS had a great influence on the reaction process of NP. As shown in Figure 9A, the study was performed in different pH ranges of 5.0 to 7.0. As the pH increases, the peak current increases first and then decreases. When pH=6, the peak current was the maximum (Figure 9B, curve a). Therefore, the pH 6.0 was selected as the optimum acidity value. Meanwhile, the peak potential gradually shifted was linearly proportional to the increase of pH (Fig. 9B, curve b).the linear regression equation was expressed as: E_{pa} = -0.06705pH + 1.008 (R=0.9975), It showed that protons has participated in chemical reactions. And 67.05mV close to the calculated theoretical value of 57.6mV, which indicates that the number of electrons transferred and the number of protons in the reaction are equal.

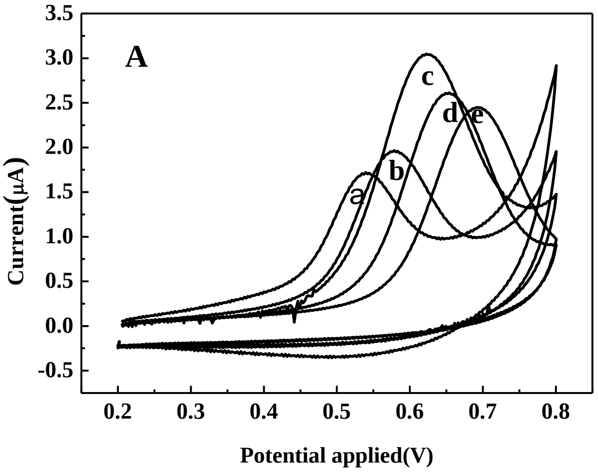

Figure 9A. The cyclic voltammograms of PBS in different pH for the determination of NP. （**a~e** : pH=5, 5.5, 6, 6.5, 7, this CV was measured in the case of NP at a concentration of 1.0 x 10^{-5} mol L^{-1}, within the potential window of 0.2-0.8 V (vs. SCE), scan rate was 100mv/s.）

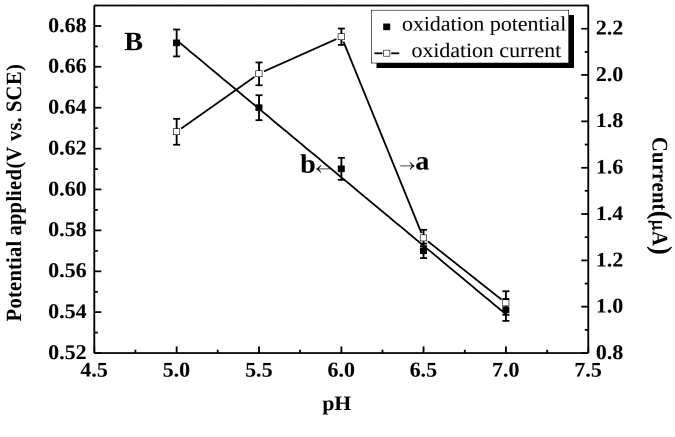

Figure 9B. The influence of different pH values on the peak current and the linear relationship with the potential (This figure was measured in the case of NP at a concentration of 1.0 x 10^{-5} mol L^{-1}, within the potential window of 0.2-0.8 V (vs. SCE), scan rate was 100mv/s.)

3.4.2 The influence of the scanning rate

The relationship between the different scanning rates and peak potential and current was investigated experimentally. Then, the electrode reaction process was discussed to further investigate the properties of AuNPs / SH-beta-CD-GR / GCE and the electrochemical behavior of NP. as the

Figure 10A shown, the oxidation peak current of NP increased with the increase of scanning rate, and here has a good linear between the oxidation peak current and the scanning rate ranges of 0.01 to 0.25 mV/s (Figure 10B), And the linear regression equation was expressed as: I_{pa}（μA）=16.79v（V/s）+ 0.2211(R=0.9937) , which indicated that the oxidation behavior of NP on AuNPs / SH-beta-CD-GR / GCE electrode was a representative adsorption-controlled process..

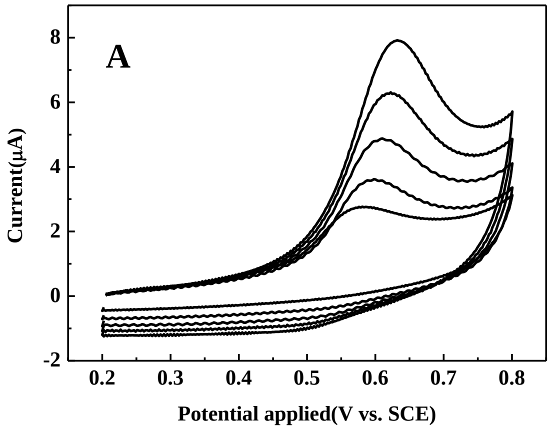

Figure10A. The cyclic voltammograms of different scan rate for the response of NP (This CV was measured in PBS (pH6.0) containing 1.0×10^{-5}mol L^{-1}NP, within the potential window of 0.2-0.8 V (vs. SCE), and the range of scan rate was from 50 to 250 mv/s.)

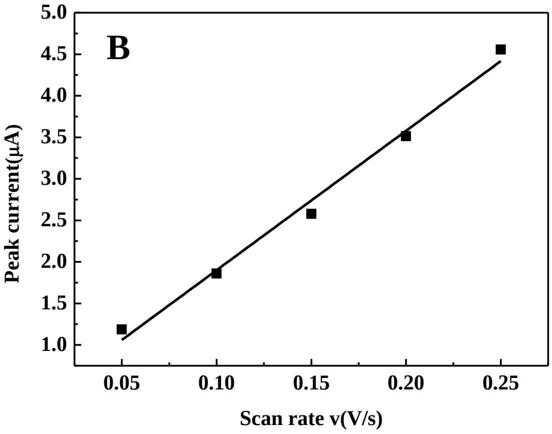

Figure 10B. The relationship between different scan rate and peak current (This figure was measured in PBS (pH6.0) containing 1.0×10−5mol L−1NP, within the potential window of 0.2-0.8 V (vs. SCE), and the range of scan rate was from 50 to 250 mv/s.)

Simultaneously, the linear relationship between the natural logarithm of potential (E_{pa}) and the scanning rate (lnv) is also well linear (Figure 10C). Which can be expressed as: E_{pa}（V）= 0.0306lnν + 0.4490 (R=0.9792) For a totally irreversible electrode process, according to the Laviron [39] , E_p is defined by the following equation:

$$E_p = E^0 + \frac{RT}{\alpha nF}\ln\frac{RTk_s}{\alpha nF} + \frac{RT}{\alpha nF}\ln\nu$$

Where E^0 is the formal standard potential, α is the charge transfer coefficient, n is the number of the electrons involved in the oxidation of NP, F is the Faraday constant (96,485 C mol^{-1}). R and T have their usual meaning. According to the slope of the E_{pa}-lnν（0.0306）, the value of αn was calculated to be 0.8392. Generally, α is assumed to be 0.5 in totally irreversible electrode process; thus, the electron transfer number is 2.

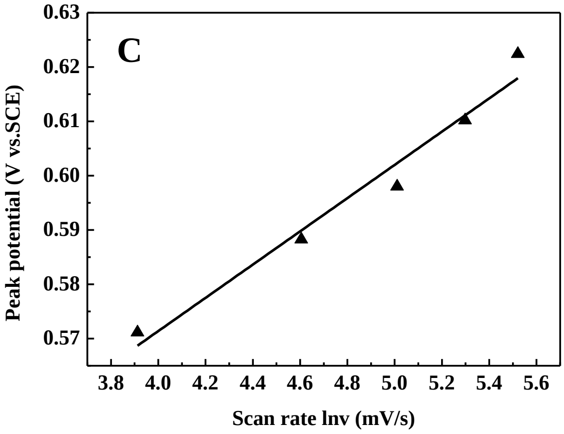

Figure 10C. The relationship between lnv and peak potential
(This figure was measured in PBS (pH6.0) containing 1.0×10^{-5}mol L^{-1}NP, within the potential window of 0.2-0.8 V (vs. SCE), and the range of scan rate was from 50 to 250 mv/s.)

3.4.3 Optimization of accumulation potential and time

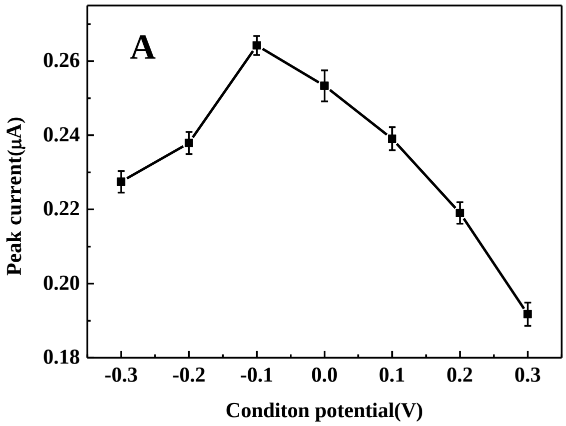

Figure 11A. The effect of accumulation potential on the peak current of NP.
(This figure was measured in PBS (pH6.0) containing 1.0×10^{-5}mol L^{-1}NP, which the range of the accumulation potential was from -0.3 to 0.3 V (vs. SCE), and scan rate was 100mv/s.)

In the experiment, the oxidation behavior of NP on AuNPs / SH-beta-CD-GR / GCE electrode was a classical adsorption-controlled process, so the accumulation potential and time were also studied. The tendency of the current about the enrichment potential and time were shown in Fig 6. As the accumulated potential increases, the peak current value improved firstly and then reduced, at -0.1V to reach the maximum.

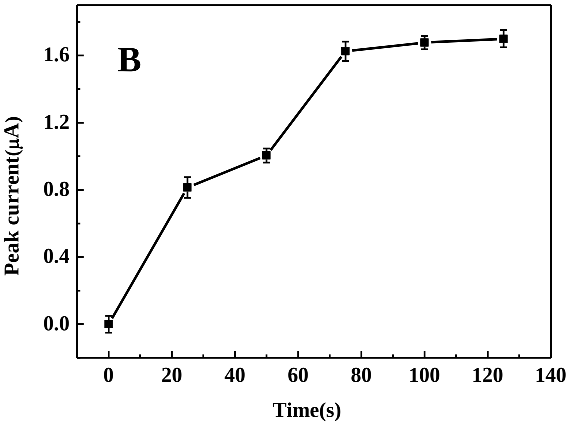

Figure 11B. The effect of accumulation time on the peak current of NP.
(This figure was measured in PBS (pH6.0) containing 1.0×10^{-5}mol L^{-1}NP, which the range of the accumulation time was from 0 to 125s, and scan rate was 100mv/s.)

Simultaneously, the peak current increased rapidly with the increase of accumulation time. When the time achieved 100 s, the response reaches a stationary value, which can be interpreted as NP to reach a saturated state on the surface of the modified electrode (Figure 11B). Thence, the optimum test conditions for NP were enriched at -0.1 V for 100 s.

3.5 Linear range and limit of detection

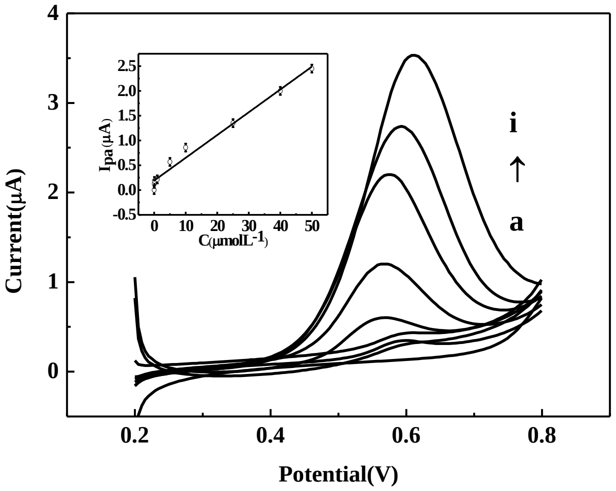

Figure12. The influence of different molar concentrations of NP (**a-i:** 0, 0.05, 0.1, 1, 5, 10, 25, 40, 50 μmol L^{-1}) on peak current. The embedded graph shows the linear relationship between the oxidation peak current and the NP concentration. (This DPV was measured in PBS (pH6.0) within the potential window of 0.2-0.8 V (vs. SCE), which the scan rate was 100mv/s and the accumulation time and potential were -0.1 V (vs. SCE) and 100s, respectively.)

Under the optimized conditions, DPV was used to investigate the relationship between the peak current and the concentration of NP. As shown in Figure 12, using the AuNPs/SH-β-CD—GR/GCE, the oxidation peak current value will be increased accordingly with the concentration increases. A linear relationship could be established between the current and the concentration of NP in the range of 0.05μmol $L^{-1}$to 50.00 μmol L^{-1} (the inset of Figure7). The linear regression equation was Ipa（μA）＝0.04592 C （μmol L^{-1}）+0.1918 (R=0.9901), and the detection limit (S/N=3) was 0.017μmol L^{-1}. As shown in Table I, compared with other modified electrodes reported in literature, the AuNPs/SH-β-CD—GR/GCE offered a reasonable linear range and a comparable detection limit.

As seen from Table 3, compared with other modified electrodes，the AuNPs/SH-β-CD-GR/GCE used in this study for the determination of NP has higher sensitivity (0.017μmolL^{-1}) and wider linear range (0.05-50μmolL^{-1}). Although the sensitivity of NGNRs-IL/GCE（0.008μmolL^{-1}），GR-DNA/GCE（0.01μmolL^{-1}）and CTAB-Fe_3O_4-rGO/GCE（0.008μmolL^{-1}）is relatively high, their linear range is narrow and discontinuous. Considering the analysis of practical samples, this method has more advantages.

Table 3. Comparison of AuNPs/SH-β-CD-GR/GCE with other modified electrodes for the determination of NP

Electrodes	**Linear range (μ molL^{-1})**	**Detection limit (μmolL^{-1})**	**References**
TiO_2/AuNPs/GCE	0.95-480.0	0.32	14
MWNT/NF/GCE	0.2-360.0	0.06	15
NGNRs-IL/GCE	0.04-6	0.008	16
GR-DNA/GCE	0.05-4.0	0.01	17
$FGNS^{IL}$/GCE	0.5 - 30 and 30 -200	0.058	18
AuNPs -CNTs /GCE	0. 05 ～ 4 and 6 ～ 14	0. 023	19
Pd/PDDA-MC /GCE	0.3- 35 and 35- 800	12.5	21
β-CD-SH-GR/Au	0.07–70.0	0.06	20
CTAB-Fe_3O_4-rGO/GCE	0.03 - 7.0 and 7.0 - 15.0	0.008	22
AuNP/PIL/GCE	0.1-120	0.033	23
CNTs-SPCEs	10 - 300	9.95	24
AuNPs/SH-β-CD/GR/GCE	0.05-50	0.017	This work

Note: GR, AuNPs, MWNT, NF, NGNRs and IL, $FGNS^{IL}$, PDDA-MC, PIL, CNTs-SPCEs are the abbreviations of graphene, gold nanomaterials, multiwalled carbon nanotubes, Nafion, nitrogen-doped graphene nanoribbons and ionic liquid, ionic liquid-functionalized graphene nanosheet ，Poly(diallyl dimethyl ammonium chloride)-mesoporous Carbon, poly(ionic liquid) hollow nanosphere, carbon nanotubes modified screen-printed carbon electrodes ,respectively.

3.6 Reproducibility, stability and interferences

On the condition of optimization, the stability and reproducibility of AuNPs / SH-β-CD-GR / GCE were determined by DPV , The relative standard deviation (RSD) of the peak current was 3.4% for 10 μmolL^{-1} NP for five consecutive measurements with AuNPs / SH-β-CD-GR / GCE. Simultaneously, the same concentration of NP was also detected by five same modified GCEs and the RSD was about 4.1%. These experiments indicated that the AuNPs / SH-β-CD-GR / GCE had an excellent reproducibility and stability. In addition, the effects of coexistence of nonylphenol in various environmental samples had been studied to evaluate the anti-interference of this method in analytical applications. Fixed NP concentration of 10μmolL$^{-1,}$ the tolerance limit for foreign species was taken as the largest amount yielding a relative error < ±5% for the determination of NP. According to the experiment results, 100-fold molar concentration of Na^+, Cl^-, Mg^{2+}, Ca^{2+}, SO_4^{2-}, Al^{3+}, K^+, Cu^{2+}, NO_3^-, 50-fold molar concentration of catechol, hydroquinone and p-nitrophenol have no interference on NP. However, 5-fold molar concentration of bisphenol A could cause the interference because its active group could be oxidized near the potential of NP. These results indicated that the present method was adequate for the determination of NP in the solutions with these interfering species except bisphenol A.

3.7 Real samples analysis

Table 4. The determination of NP in samples

Samples	**Added (μM)**	**Found (μM, n=3)**	**RSD (%)**	**Recovery (%)**
Industrial wastewater	10	10.59	4.16	105.9
	9	8.89	3.36	98.81
canal water	10	10.12	1.33	101.2
	9	8.65	4.39	96.11

As shown in Table 4, the AuNPs/SH-β-CD—GR/GCE was applied to analyze the contents of NP in industrial wastewater collected from Chemical Plant of Chengdu China and canal water Gathered from the main campus of Chengdu University of Technology, China by standard addition method to further evaluate the applicability of this fabricated electrode. Each sample solution was subjected to three parallel determinations, and the detection recovery rate of real samples is over the range of 96.11% to 105.9%, indicating that the recovery rate of the method was good and can be quantitatively analyzed in actual samples.

4. CONCLUSIONS

In this work, a AuNPs/SH-β-CD—GR composite film-modified GCE was prepared and utilized as the electrochemical sensor for the determination of NP. Meanwhile, the electrochemical behavior of NP on the surface of AuNPs/SH-β-CD—GR/GCE was studied by CV and DPV. Comparison between the AuNPs/SH-β-CD—GR/GCE with other electrodes such as bare GCE, AuNPs / GCE and AuNPs / GR / GCE, The former improved the absorption and electrocatalytic oxidation activity of NP. Moreover, the oxidation peak current of NP on the modified electrode is greatly increased and the detection limit is 0.017μmol L^{-1}, which has offered a wider linear range, a lower detection limit and a higher sensitivity when it's under the optimal conditions. This indicates that the modified electrode had a lot of potential uses in environmental sample analysis.

References

1. W.S. Zhou, B. Zhao, X.H. Huang and X.D. Yang, *Chin. J. Anal. Chem.*, 41 (2013) 675.
2. O. Varisli, C. Uguz, C. Agca, Y. Agca, *Reprod. Toxicol.*, 28 (2009) 542.
3. H.B. Lee, T.E. Peart, *Anal. Chem.*, 67 (1995) 1976.
4. L.M. Mcclusky, J.C. De, M.S Bornman, *Toxicol. Sci.*, 95 (2007) 249.
5. M.C. Pietrogrande, G. Basaglia, *Trend. Anal. Chem.*, 26 (2007).
6. K. Inoue, Y. Yoshimura, T. Makino, H. Nakazawa, *Analyst*, 125 (2000) 1959.
7. L. Nú˜nez, E. Turiel, J.L. Tadeo, *J. Chromatogr. A.*, 1146 (2007) 157–163.
8. T. Raecker, B. Thiele, R.M. Boehme, K. Guenther, *Chemosphere*, 82 (2011) 1533.
9. A. Latorre, S. Lacorte, D. Barceló, M. Montury, *J. Chromatogr. A.*, 1065 (2005) 251.
10. J.W. Park, S. Kurosawa, H. Aizawa, Y. Goda, M. Takai, K. Ishihara, *Analys*t, 131 (2006) 155.
11. J.H. Li, D.Z. Kuang, Y.L. Feng, F.X. Zhang, Z.F. Xu, M.Q. Liu, *J. Hazard. Mater.*, 250 (2012) 201.
12. H.S. Yin, Y.L. Zhou, S.Y. Ai, Q.P. Chen, X.B. Zhu, X.G. Liu, L.S. Zhu, *J. Hazard. Mater.*, 174 (2010) 236.
13. W.J.R. Santos, P.R. Lima, A.A. Tanaka, S.M.C.N. Tanaka, L.T. Kubota, *Food.Chem.*, 113 (2009) 1206.
14. J.D. Huang, X.M. Zhang, S. Liu, Q. Lin, X.R. He, X.R. Xing, W.J. Lian and D. Tang, *Sensor. Actuat. B.*, 152 (2011) 292.
15. J. Zhang, Y.H. Niu, S.J. Li, R.Q. Luo and C.Y. Wang, *Sensor. Actuat. B.*, 193 (2014) 844.
16. Y.H. Pan, L. Shang, F.Q. Zhao, B.Z. Zeng, *Electrochimica. Acta.*, 151(2015) 423.
17. L.X. Zeng, A. Zhang, X.H. Zhu, C.Y. Zhang, Y. Liang and J.M. Nan, *J. Electroanal. Chem.*, 703 (2013) 153.
18. X. Meng .Meng, H.S.Yin, M. Xu, S.Y.Ai, J.Y. Zhu, Journal of Solid State Electrochemistry, 16 (2012) 2837.
19. Q.L. Zheng, P. Yang, S.J. Xu, Journal of Instrumental Analysis, 31 (2012) 273.
20. F. Xue, Z.Y. Gao, X.M. Sun, Z.S. Yang, L.F. Yi and W. Chen, *J. Electrochem. Soc.*, 162 (2015) H338.
21. C. Ma, Z.X. Zheng, J.J. Liu, J. Li, C.M. Wang, Journal of The Electrochemical Society, 162 (2015) H816.
22. J. Zou, M.L. Guo, Y.L. Feng, M. Yang, Y.J. Cao, D.B. Zhu, Y. Yu, Microchimica Acta, 184 (2017) 533.
23. J. Ren, J. Gu, L. Tao, M. Yao, X. Yang, Analytical Methods, 7 (2015) 8094.
24. M. Buleandra, A.A. Rabinca, E.C. Mitran, A.A. Ciucu, Materiale Plastice, 53 (2016) 491.
25. M.A. Mohammad, D.F. Afsaneh, A.S.M. Mohammad, B. Ali, F.M. Bi-Bi, Z. Reza, *Measurement*, 62 (2015) 88.
26. A. Daryoush, Z. Somaye, F. Fariba, M. Ali, *Mater. Sci. Eng*. C., 43 (2014) 97.
27. M.E.N. Rasha, *Talanta*, 96 (2012) 161.
28. L.H. Tang, Y. Wang, Y.M. Li, H.B. Feng, J. Lu, J.H. Li, *Adv. Funct. Mater.*, 19 (2009) 2782.

29. K.S. Kim, Y. Zhao, H. Jang, S.Y. Lee, J.M. Kim, K.S. Kim, J.H. Ahn, P. Kim, J.Y. Choi, B.H. Hong, *Nature*, 457 (2009) 706.
30. K. Zhang, V. Dwivedi, C.Y. Chi, J.S. Wu, *J. Hazard. Mater.*, 182 (2010) 162.
31. M. Zhou, Y.M. Zhai, S.J. Dong, *Anal. Chem.*, 81 (2009) 5603.
32. Y. Zhang, R. Yuan, Y.Q. Chai, W.J. Li, X. Zhong and H.A. Zhong, *Biosens. Bioelectron.*, 26 (2011) 3977–3980.
33. K.S. Liu, H.G. Fu, Y. Xie, L.L. Zhang, K. Pan and W. Zhou, *J. Phys. Chem. C.*, 112 (2008) 951.
34. J.X. Zhang and P.X. Ma, *Adv. Drug. Deliv. Rev.*, 65 (2013) 1215.
35. M.E. Davis, *Mol. Pharm.*, 6 (2009) 659.
36. X.H. Zhu, Q.F. Jiao, X.X. Zuo, X. Xiao,Y. Liang and J.M. Nan, *J. Electrochem. Soc.*, 160 (2013) H699.
37. X.Y. Lin, Y.N. Ni, S. Kokot, *Analytica Chimica Acta*, 765 (2013) 54.
38. P. Diao, D.F. Zhang, M. Guo, Q. Zhang, *Journal of Catalysis, 250* (2007) 247.
39. E. Laviron, *J. Electroanal. Chem.*, 52 (1974) 355.